

Vertical Array Records during 2007 Niigata-Ken Chuetsu-Oki Earthquake and Incident Wave Energy

T. Kokusho¹ and T. Suzuki²

¹ Professor, Dept. of Civil Engineering, Chuo University, Tokyo, Japan

² Graduate Student, Ditto

Email: kokusho@civil.chuo-u.ac.jp

ABSTRACT :

During the 2007 Niigata-ken Chuetsu-oki earthquake, a very strong motion was recorded by a vertical array seismic observation system in the TEPCO nuclear power plant, which clearly indicated soil nonlinearity effect. In this paper, time histories, response spectra and Fourier spectrum ratios of the recorded motions are shown and their characteristics are discussed. Then, soil properties for the main shock are back-calculated and compared, indicating a great degree of strain-dependent nonlinearity in sand dune layer. Finally, based on the results, seismic wave energy propagating upward by SH-wave is calculated to compare with that of other earthquakes. The incident energy at the base rock was 434 kJ/m² and 73% of the energy was in the frequency range lower than 1.0 Hz, indicating the earthquake gave great impact on soil ground and backfill.

KEYWORDS: strong motion records, vertical array, soil nonlinearity, wave energy, soil settlement

1. INTRODUCTION

The Niigatoken Chuetsu-Oki earthquake ($M_J=6.8$), which occurred in July 16, 2007 along the coast of Japan Sea, attacked a relatively narrow region encompassing Kashiwazaki city and Kariwa village of Niigata prefecture with very strong intensity of shaking. Although the epicenter was a few kilometer off the coast, the causative fault (the reverse thrust with the strike N 30 ° E) reached the land area. The Kashiwazaki-Kariwa Nuclear Power Plant (KK-NPP), the largest NPP in the world owned by Tokyo Electric Power Company (TEPCO), was situated in the focal area along the coast and experienced strong shaking exceeding the design acceleration spectra by 2-3 times at the maximum. Despite that, all the nuclear reactors under operation were stopped safely and cooled down without significant leakage of radioactive materials. In a good contrast to that, considerable settlement occurred in backfill soils around important buildings embedded on bedrock, buried conduits, etc, causing various damage in non-nuclear structures. The seismic design of these non-nuclear normal structures was regulated in accordance to a criteria for general civil engineering structures.

In this paper, strong motion records obtained by a set of accelerometers installed inside the NPP are incorporated to characterize ground motions and soil response. Vertical array records in the NPP site is back-calculated to optimize soil properties exhibited during the main shock and aftershocks to compare among them. Finally, the incident wave energy will be evaluated based on the records and back-calculated soil properties to characterize the incident seismic wave in terms of energy.

2. EARTHQUAKE RECORDS AND SITE PERFORMANCE

Fig.1 is the satellite photograph of the area strongly affected by the earthquake. The KK-NPP was located along the coast of the



Figure.1 Damaged area along the coast of Sea of Japan (Google Map).

Japan sea and about 4 km far from the center of Kashiwazaki city. Strong motion records were obtained by many accelerometers installed at the surface and depth in the plant site. In addition, a K-net station near the center of Kashiwazaki city which had been deployed by NIED (National Research Institute for Earth Science and Disaster Prevention) in Tsukuba, Japan, obtained the record at the ground surface.

The surface soil layer of the K-net site consists of relatively dense dune sand of about 18 m thick followed by Pleistocene stiff clay of 45 m thick, which are underlain by Tertiary mudstone. Fig. 2 shows the acceleration time histories of the K-net Kashiwazaki in EW and NS directions. A very peculiar shape of waves can be recognized in the acceleration time histories, which reflects the cyclic mobility of saturated sand cyclically sheared by seismic wave under undrained condition, indicating that the dune sand was not loose enough to fully liquefy.

Fig.3 shows a plan view of the KK-NPP with 7 units of the power station. Fig.4 shows the typical geological cross-section of the 7 units. The geology of the site is basically similar to that of Kashiwazaki K-net and consists of dune sand at the top underlain by Pleistocene soil and Tertiary mudstone. Nuclear-related important facilities of the stations, such as reactor buildings (RB) and turbine buildings (TB), were all embedded directly on the rock and backfilled by the dune sands.

The accelerometers had been installed at many locations in the NPP site, on the surface and depth of the ground and inside the structures, though not all of them could record the time history of the main shock. The vertical array investigated herein in detail was deployed near Service Hall slightly far from the power units and on the top of a sand dune. All accelerometers plotted in Fig.3 are 3-dimensional, EW, NS and UD, though the horizontal directions are not the true EW/NS directions but modified by 19 degrees according to the plant units alignment (named here as PEW/PNS) as shown in Fig.3. It should be pointed out here that the ground motion during the main shock was obviously larger in the PEW direction than in the PNS direction presumably due to the fault rupture mechanism.

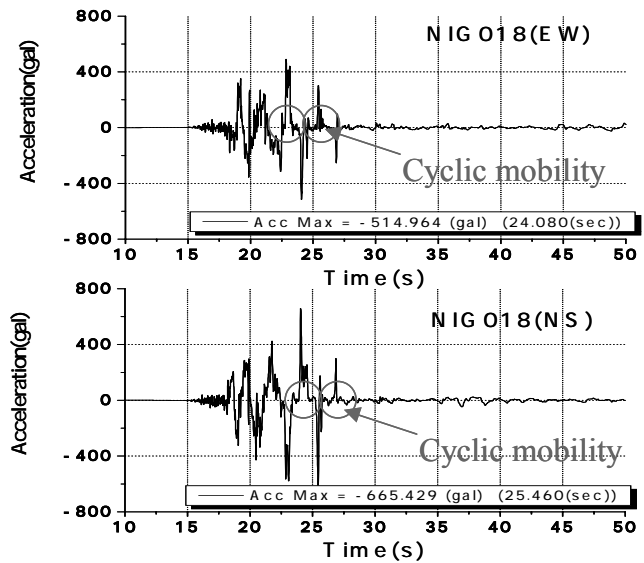


Figure 2 Acceleration records of K-net at Kashiwazaki city showing cyclic mobility

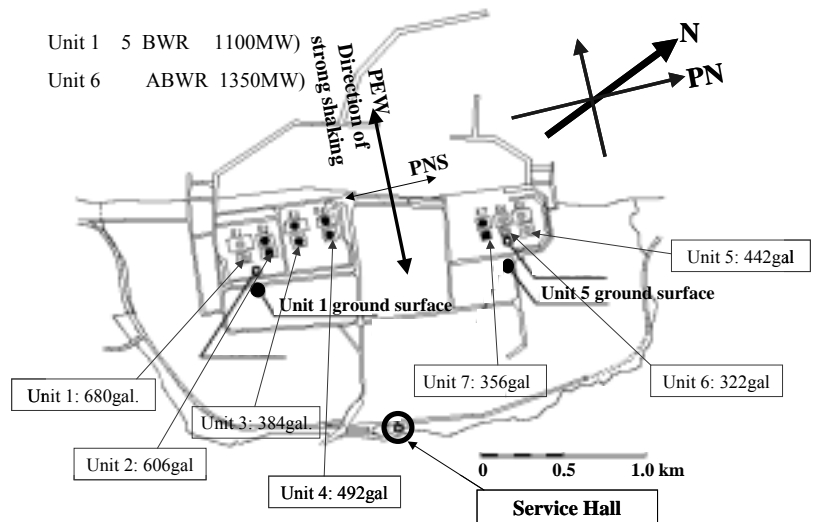


Figure 3 Plan view of Kashiwazaki-Kariwa NPP and measured max. Acc. at RB foundations of 7 units.

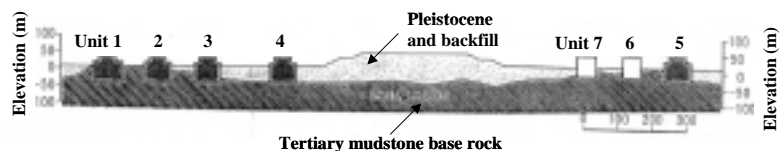


Figure 4 Geological cross section of 7 RB buildings embedded on bedrock in Kashiwazaki-Kariwa NPP.

Fig.5 shows the acceleration response spectra of 5% damping ratio in the PEW direction records obtained on the deeply embedded concrete RB foundations of the 7 units superposed on the same chart. As a whole, the peak periods of the acceleration spectra are unexpectedly long indicating a great involvement of long period ground motions. Actually, if the response spectrum of the same motion is expressed in terms of velocity, the peak period is as large as 3 seconds. The long period motion seems responsible for the large subsidence of backfill soils, because the longer the period, the larger effect of cyclic shear stress can transmit to deeper level of the ground. Also noted is that the response of one group (Units 1-4) is apparently larger than that of the other group (Units 5-7), which are located by 1 km north.

Fig.6 compares the acceleration spectra between the RB foundations and the neighboring ground surface for Units 1 and 5, where the time histories on the ground were successfully recorded. The spectrum is obviously larger on the ground surface than on the foundation, demonstrating the effect of the embedded concrete foundation directly resting on the base rock. This effect is particularly conspicuous for short period range of $T \approx 0.5$ s or less, which seems to have been beneficial to mechanical equipments of the plant facilities.

In Fig.7, the measured acceleration time histories in Unit 1 on the foundation and the ground are integrated twice in terms of time to have velocities and displacements, respectively. The ground velocity time history shown at the top row looks apparently strange in the latter part of the motion, probably reflecting the residual displacement of the base mat of the accelerometer, the occurrence of which was actually confirmed after the earthquake. The displacements calculated from the first part of the velocity motions, exempt from the subsequent residual offset, shown at the bottom of Fig.7, indicates that large displacement between foundation and ground was induced during the major shaking. Though its absolute value may not be so accurate because the ground surface motion was measured at a place about 200m far from the RB foundation, the qualitative trend seems sufficiently reliable, implying that the maximum relative displacement occurred by the ground movement westward (seaward) relative to the foundation.

In the authors' opinion, this relative displacement, in addition to the cyclic shear stress, made a great contribution to the settlement of the backfill soils in addition to the effect of the long period motion as previously mentioned. The settlement was particularly large at the seaside of the buildings compared to the inland side. At the seaside it was 1.6 m maximum because the ambient soil was apt to separate from the structure, while in the inland side, even some compression

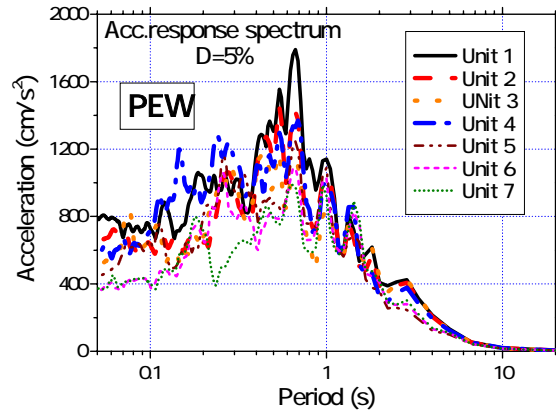


Figure 5 Acceleration response spectra in the PEW direction on RB foundations of 7 units.

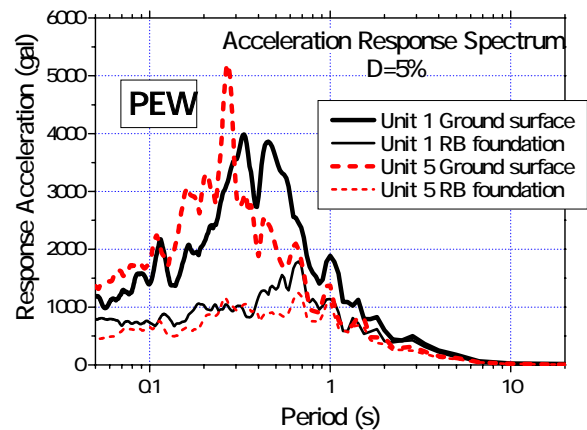


Figure 6 Acceleration spectra between the RB foundations and the neighboring ground surface for Units 1 and 5.

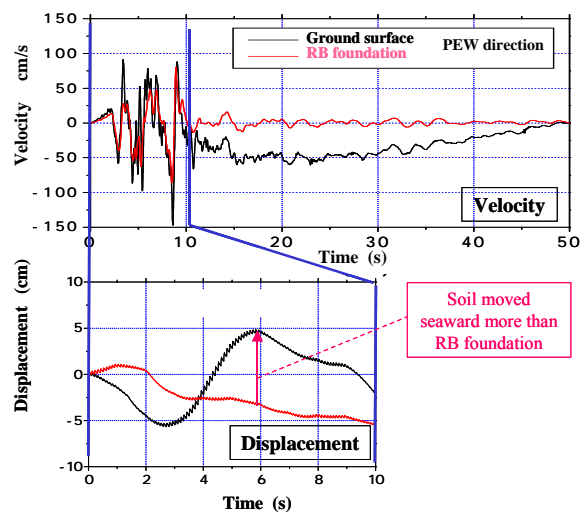


Figure 7 Velocity and displacement for ground surface compared to RB foundation.

while in the inland side, even some compression

heave could be observed at some locations.

3. VERTICAL ARRAY RESPONSE IN NPP SITE

A vertical array installed at Service Hall on the top of the sand dune in the KK-NPP site (See Fig.3) consists of 4 down-hole accelerometers at the depth of GL-2.4 m, GL-50.8 m, GL-99.4 m and GL-250 m as depicted in Fig.8. The top 2 are in the sand dune layer of 83 m thick and the bottom 2 are in the Tertiary mudstone. The water table is judged to be at GL-45 m because the P-wave velocity shown in the figure jumps to the value exceeding $V_p=1500$ m/s, there.

Acceleration time histories at the 4 levels in PEW direction during the main shock are shown in Fig.9. Corresponding acceleration response spectra for $D=5\%$ are shown in Fig.10 (a), indicating that the long period motion of $T>0.5$ s tends to amplify in the interval of 250 m thick, whereas the motion shorter than that clearly

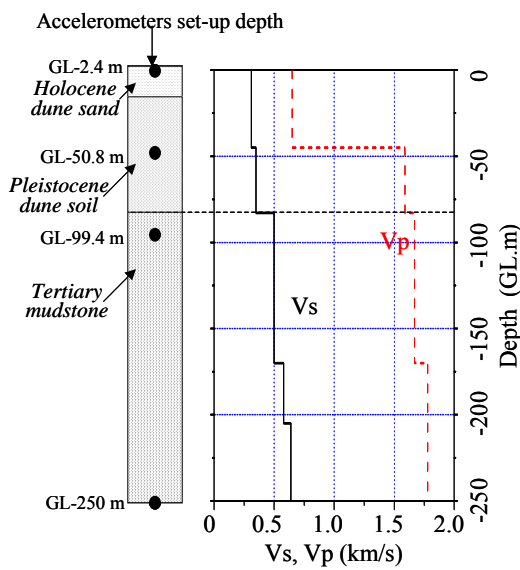


Figure 8 S-wave velocity and other profiles at the vertical array site.

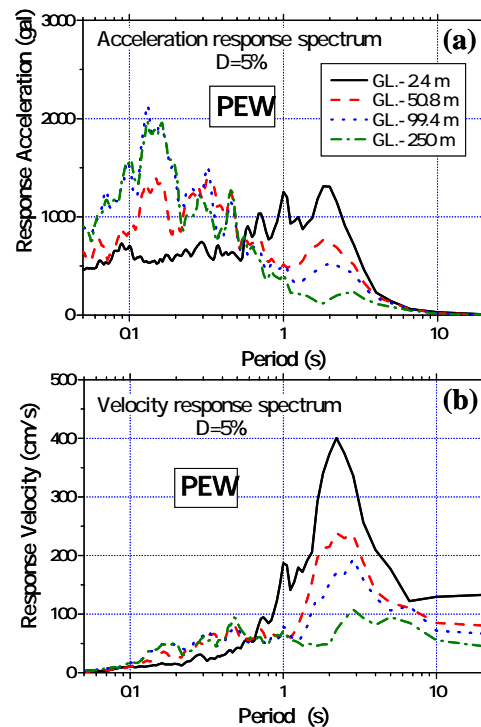


Figure 10 Response spectrum for acceleration (a) and velocity (b) of vertical array records in PEW direction

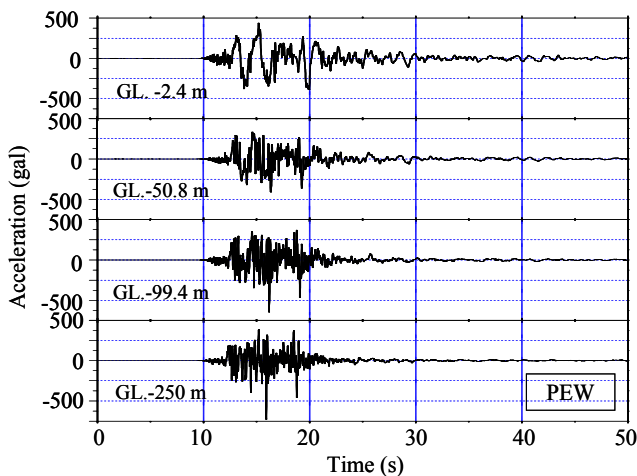


Figure 9 Acceleration time history of vertical array in PEW direction.

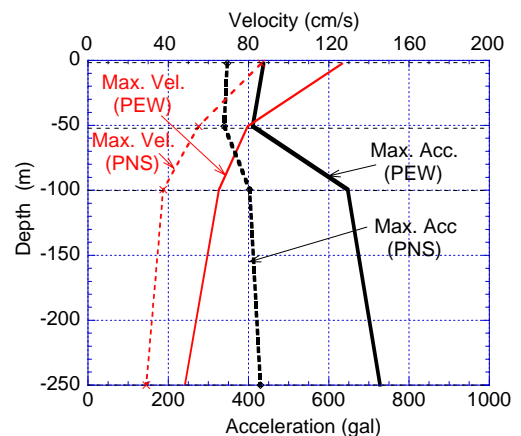


Figure 11 Maximum acceleration and velocity along depth in vertical array.

deamplify in the sand dune. The corresponding velocity response spectra for $D=5\%$ of PEW direction in Fig.10 (b) indicate that the spectrum peak longer than 2 s is considerably amplified continuously from the bottom to the top. The down-hole distributions of maximum acceleration and maximum velocity in the horizontal direction are depicted in Fig.11. Reflecting the frequency-dependent characteristics in the response spectra in Fig.10, a clear trend of deamplification in acceleration and amplification in velocity can be seen.

Fourier spectrum ratios were calculated between the surface motion and the down-hole motions of different levels. Fig.12 exemplifies one for the PEW direction between the surface (GL.-2.4 m) and GL.-99.4 m, in which not only the main shock but also aftershocks are shown with the average curve and its standard deviation for 5 shocks. An obvious difference in the amplification can be recognized between the main shock and the aftershocks. The frequency of the first peak in the spectrum ratio tends to be lower in the main shock, and higher order peaks in the aftershocks become obscure in the main shock. These differences may be largely attributable to strain-dependent soil properties in the layer above the mudstone bedrock.

Back-calculation was carried out to evaluate the nonlinear soil properties by using Extended Bayesian Method (Honjo et al. 1998, Kokusho et al. 2005). Based on a 1D soil model constructed from soil profiles provided by TEPCO, S-wave velocity V_s and damping ratio D of individual layers are optimized from initial values of guess to have the best fit with the observed spectrum ratios. The details of the back-calculation procedures are available by Kokusho et al. (2005). Fig.13 exemplifies the optimized spectrum ratio of GL.-2.4 m/GL.-99.4 m in PEW direction compared with the observation and also with the initial guess. Though the optimized spectrum ratio does not match the observation so perfectly, it is closer than that using the initial small-strain properties.

In Fig.14 (a), the distribution of the back-calculated values of V_s and D are drawn versus the depth for PEW and PNS directions together with corresponding small strain V_s given by in situ S-wave logging tests V_{s0} . Compared to the small strain values, the back-calculated values of V_s for the main shock decrease by 37-23% in the soil layers and by 2-0.4% in the Tertiary underlying mudstone. The damping ratios D shown in Fig.14(b) are evaluated as 17-14% in the soil layers, which are considerably larger than estimated small strain values D_0 depicted in the figure, while in the rock they are as small as 1.5-1% not so different from the value of D_0 . Thus remarkable nonlinearity in properties took place in soil layers whereas the effect remained marginal

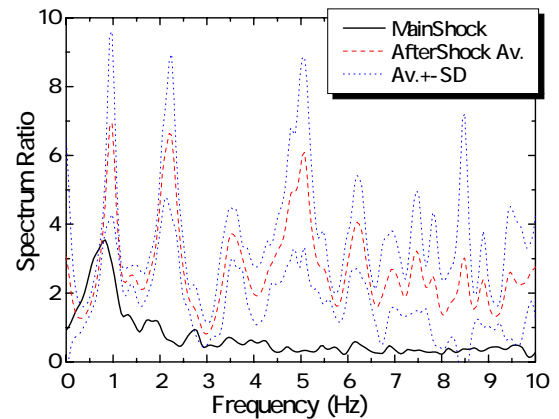


Figure 12 Spectrum ratio between surface and GL.-99.4 m in PEW direction for main shock and aftershocks.

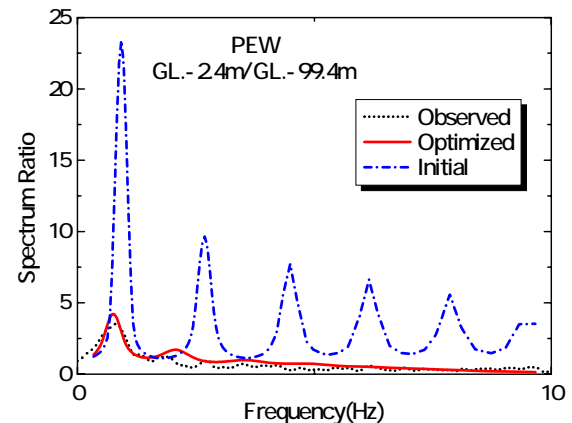


Figure 13 Optimized Spectrum ratio between surface and GL.-99.4 m in PEW direction for main shock compared to observation

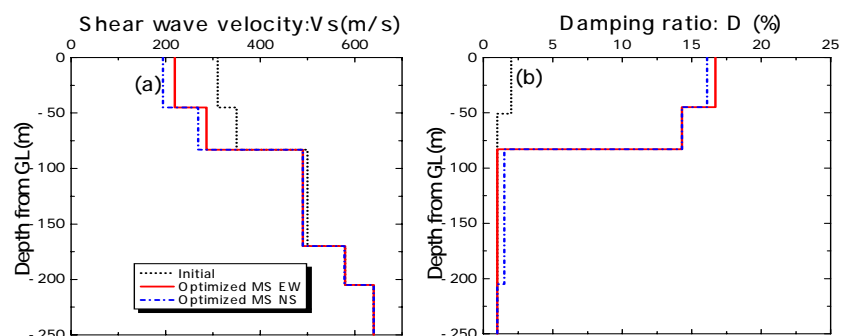


Figure 14 Optimized S-wave velocity and damping ratio for main shock along depth.

Thus remarkable nonlinearity in properties took place in soil layers whereas the effect remained marginal

in the base rock. The maximum induced strain calculated by a forward multi-reflection analysis using the optimized properties was 0.27 % for the soil layers and about 0.14% for the rock.

4. EVALUATION OF INCIDENT SEISMIC WAVE ENERGY

Considering that the energy is directly related to induced strain or damage in superstructures (Kokusho et al. 2007), it is desirable to evaluate a seismic input not only by acceleration or velocity but also by energy. The seismic wave energy E , if its major portion is assumed to be transported by SH-wave, can be calculated simply as

$$E = \rho V_s \int (\dot{u})^2 dt \quad (1)$$

where \dot{u} is particle velocity of horizontal motion and ρV_s is the seismic impedance of a layer where the wave is defined. Note that \dot{u} in Eq.(1) is the particle velocity not directly of recorded motions but of traveling waves in either upward or downward direction. Therefore, it is essential to separate a measured motion at a point into upward and downward waves in order to evaluate the individual energies (Kokusho and Motoyama 2002).

If a site consists of a set of horizontal soil layers and they behave as linear materials, upward and downward waves at any point can be calculated from a surface record based on the multiple reflection theory (Schnabel et al., 1972) from which the flow of the energy there is readily evaluated. During strong earthquakes, seismic motions at the ground surface are very much influenced by the soil nonlinearity. However, the deeper the soil is, the more linearly soil behaves even during strong earthquakes (Kokusho et al., 1996). If vertical array records are available, the energy flow in deeper ground can be evaluated by using earthquake records at deeper levels where seismic wave is less contaminated by soil nonlinearity. The separation of upward and downward waves from measured motions at two different underground levels is readily made using the multiple reflection theory as explained in another literature (Kokusho and Motoyama, 2002). On the other hand, the upward energy at a ground surface can be calculated by substituting a half of particle velocity there into \dot{u} in Eq.(1).

The energies evaluated at GL-99.4 m, almost the same elevation as the embedded foundations of the reactor buildings RBs), using the optimized properties are depicted in Fig.15 together with the corresponding velocity time histories. The upward energy increases monotonically with time and amounts to be 351 kJ/m² in PEW direction and 83 kJ/m² in PNS direction eventually. The total incident energy at GL.-250 m, GL.-99.4 m, GL.-50.8 m and at GL.-2.4 m are 453 kJ/m², 434 kJ/m², 384 kJ/m² and 377 kJ/m², showing a gradually decreasing trend with decreasing depth. These values are larger than the incident wave energy at the deepest level (GL.-83.4 m) of the vertical array in Port Island (305 kJ/ m²) during the 1995 Kobe earthquake (Kokusho and Motoyama 2002).

Though seismically induced strain or damage of structures is highly dependent on the incident wave energy, another important damage-related parameter is the frequency content of the incident energy. In order to know the frequency-dependent energy distributions, the energy spectrum is proposed herein as the power spectrum of the particle velocity times the seismic impedance. Thus, the total energy defined in Eq.(1) can be expressed as the sum of energy spectra, $\rho V_s T (A_k^2 + B_k^2) / 2$ corresponding to frequencies, $f_k = k \Delta f$; as

$$E = \rho V_s \int (\dot{u})^2 dt = \rho V_s \Delta t \sum_{m=0}^{N-1} x_m^2 = \rho V_s T \left[\left(\frac{A_0}{2} \right)^2 + \frac{1}{2} \sum_{k=1}^{N/2-1} (A_k^2 + B_k^2) + \left(\frac{A_{N/2}}{2} \right)^2 \right] \quad (2)$$

where velocity time history consisting of m discrete data is expressed by the finite Fourier series with coefficients A_k and B_k , and $\Delta f = 1/(N \Delta t)$, $k = 0, 1, 2, \dots, N/2$, $\Delta t =$ time increment of the velocity time

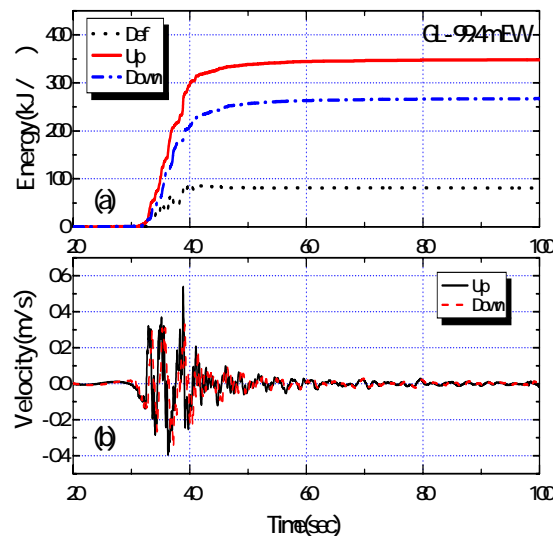


Figure 15 Time histories of wave energies (a) and particle velocities of upward & downward waves (b) at GL.-99.4 m.

history, N = the total data points in time history, and $T = N\Delta t$.

The energy spectrum at GL.-99.4 m is shown in Fig.16, where, needless to say, the sum of the individual spectrum amplitudes is equal to the total energy (434 kJ/m²) in the PEW and PNS directions at GL.-99.4 m. Note that a major portion (73%) of the incident wave energy during the 2007 Chuetsu-Oki earthquake is in the frequency range lower than 1.0 Hz, indicating that the earthquake gave much stronger impact on soil ground and soil structures than on superstructures with higher resonant frequencies as previously mentioned.

In both Fig.17, the total energy at GL.-99.4 m is plotted with a large star symbol versus the focal distance of the main shock (23 km according to TEPCO). The solid line in the chart indicates the energy per unit area calculated by simple equations

$$E_{IP}/A = E_0 / (4\pi R^2) \quad (3)$$

where E_0 is the total wave energy released from a point source and is determined using the empirical equation by Gutenberg (1955):

$$\log E_0 = 1.5M + 11.8 \quad (4)$$

Here, E_0 has units of ergs (1 erg = 10⁻¹⁰ kJ), M is the earthquake magnitude using the Richter scale. Here the Japanese Earthquake Magnitude, M_J , was used to compute E_0 because the Richter and Japanese magnitude scales are almost equivalent. Thus, input energies E_{IP} at bedrock during the earthquake may be readily computed by Eqs.(3) and (4), given earthquake magnitude and focal distances.

Incident energies at base layers 100–300 m deep from GL computed from the KiK-net down-hole array records during the 2004 Niigataken Chuetsu earthquake ($M_J = 6.8$) are also compared in Fig.17 with the same theoretical solid line (Kokusho et al. 2006). In the same chart, incident energies at base layers around 100 m deep during the 1995 Kobe earthquake ($M_J = 7.2$) are also plotted and compared with the theoretical dashed line by Eqs.(3) and (4) (Kokusho et al. 2006). The energy during the Chuetsu-Oki earthquake was evidently higher in the near fault region than the 2004 Chuetsu earthquake of the same magnitude. It is also obvious that the energy in the NPP site was as high as in the Kobe earthquake despite that the magnitude was smaller. One of the reasons seems to be attributable to the fault mechanism of the Chuetsu-Oki earthquake such as directivity and asperity in relation to the NPP site.

5. CONCLUSIONS

The ground motions obtained at KK-NPP during the Chuetsu-Oki earthquake and some analyses based on them yielded the following major findings;

- (1) Peak periods of the acceleration spectra are unexpectedly long indicating a great involvement of long period motions with the peak period of 3 seconds in the velocity response spectrum, which seems responsible for the large subsidence of backfill soils in the NPP site by introducing large cyclic shear stress or strain into deeper soils.
- (2) Displacements calculated from the motions on the RB foundation resting on the bedrock and neighboring soil surface indicate that horizontal ground displacement occurred westward (seaward) relative to the foundation, which may have contributed to considerable settlement of the backfill soils around NPP important buildings particularly large at the seaside compared to the inland side.

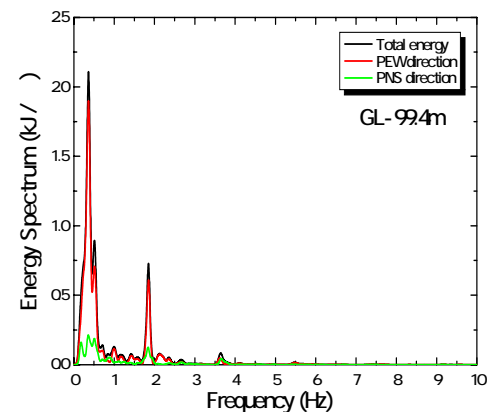


Figure 16 Energy spectrum of incident wave at GL.-99.4 m.

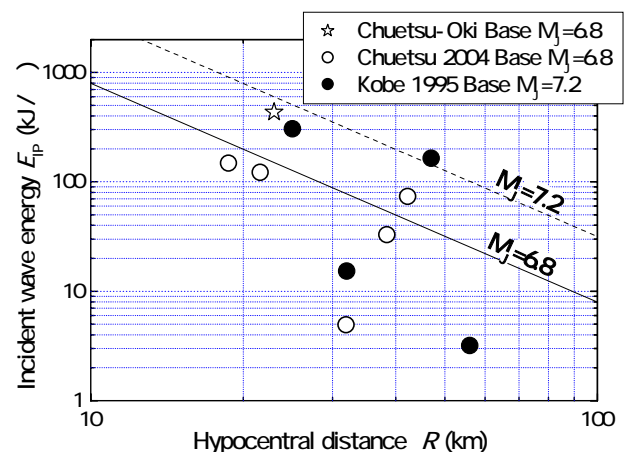


Fig.17 Incident wave energy versus hypocentral distance evaluated from vertical array records compared with simple calculation based on spherical energy dissipation.



- (3) Main shock motions measured in the vertical array at the top of the sand dune indicates deamplification in acceleration and amplification in velocity as the records approach to the ground surface. Back-calculation of the motions indicates that remarkable nonlinearity in properties took place in soil layers whereas the effect remained marginal in the underlying base rock.
- (4) The incident wave energies evaluated at almost the same elevation as the RB foundations amounts to be 434 kJ/m². The energy spectrum proposed and evaluated here indicates that a major portion (73%) of the incident wave energy was in the frequency range lower than 1.0 Hz, indicating the major energy involved in long period motions gave great impact on soil ground and backfill.
- (5) The incident wave energy at the RB foundation was larger than that of the 2004 Chuetsu earthquake of the same magnitude and also almost equivalent to that of the 1995 Kobe earthquake of the larger magnitude.

ACKNOWLEDGMENTS

TEPCO (Tokyo Electric Power Company) is gratefully appreciated for disseminating the valuable strong motion records during the 2007 Niigataken Chuetsu-Oki earthquake. NIED (National Research Institute for Earth Science and Disaster Prevention) in Tsukuba, who generously provided K-net and KiK-net data through the internet, is gratefully acknowledged. The great efforts in data reduction of voluminous KiK-net records by graduate and undergraduate students of Civil Engineering Department in Chuo University are also very much appreciated.

REFERENCES

- Gutenberg, B. (1955): The energy of earthquakes, *Quarterly Journal of the Geological Society of London*, Vol.CXII, No.455, 1-14.
- Honjo, Y. Iwamoto, S., Sugimoto, M., Onimaru, S. & Yoshizawa, M. (1998): Inverse analysis of dynamic soil properties based on seismometer array records using the Extended Bayesian method. *Soils and Foundations*: Vol.38, No.1, 131-143.
- Kokusho, T., Matsumoto, M. and Sato, K. (1996): "Nonlinear seismic properties back-calculated from strong motions during Hyogoken-Nambu EQ." Proc. World Conference on Earthquake Engineering (Acapulco), CD-publication.
- Kokusho, T. and Motoyama, R. (2002): "Energy dissipation in surface layer due to vertically propagating SH wave." *Journal of Geotechnical and Geoenvironmental Engineering*, ASCE, Vol.128, No.4: 309-318.
- Kokusho, T., Aoyagi, T. and Wakunami, A. (2005): In situ soil-specific nonlinear properties back-calculated from vertical array records during 1995 Kobe Earthquake, *Journal of Geotechnical and Geoenvironmental Engineering*, ASCE, Vol.131, No.12, 1509-1521.
- Kokusho, T., Motoyama, H. and Ishizawa, T. (2006): Seismic wave energy in surface layers and energy-based damage evaluation", Proc. 8th National Conference on Earthquake Engineering in commemorate of 100th San Francisco Earthquake, San Francisco, 8NCEE-133, CD-publication.
- Kokusho, T., Motoyama, R. and Motoyama, H. (2007): Wave energy in surface layers for energy-based damage evaluation, *Soil Dynamics & Earthquake Engineering* 27, 354-366.
- Schnabel, P. B., Lysmer, J. & Seed, H. B.(1972): "SHAKE, A computer program for earthquake response analysis of horizontally layered sites." *Report EERC 72-12*, University of California Berkeley.